



EFFECTS OF HORIZONTAL / VERTICAL FIN TIP GAPS ON MICROCHANNEL HEAT SINKS PERFORMANCE IN ELECTRONIC COOLING

H. J. Tony Tan* and M.Z. Abdullah

School of Mechanical Engineering, Universiti Sains Malaysia
Engineering Campus, 14300 Nibong Tebal, Penang, Malaysia
tonytan89@hotmail.com, Phone: +60164229648

(Geliş Tarihi: 28. 06. 2011, Kabul Tarihi: 12. 03. 2012)

Abstract: This study focuses on the effect of vertical and horizontal fin tip gaps on microchannel heat sink performance. Three different fin configurations (rectangular, triangular, and trapezoidal) of the microchannel heat sink have been designed in three-dimensional models with different vertical fin tip gaps. The finite volume method has been applied to solve the governing equations in order to simulate microchannel heat sink performance. The solution is executed using Gambit 2.3.26/FLUENT 6.3.26 software. In the small vertical fin tip gap of $V_g/W_c < 0.8$, the rectangular fin heat sink shows a small decrease in thermal resistance and thus achieves the minimum thermal resistance at $V_g/W_c = 0.8$. However, the trapezoidal fin shows a constant thermal resistance in the smaller fin tip gap of $V_g/W_c \leq 0.4$, which then increases substantially at $V_g/W_c > 0.4$. Comparatively, the triangular fin heat sink shows continuous increments in thermal resistance in all ranges of the vertical fin tip gap. The existence of the small vertical fin tip gap does not deteriorate heat sink thermal performance; instead, it results in performance improvement, especially in the case of the rectangular fin heat sink. The rectangular fin heat sink is analyzed further with regard to the effect of the horizontal fin tip gap with the introduction of horizontal fins on both sides of each vertical fin. The heat sink thermal resistance is significantly reduced with the existence of the optimum horizontal ($H_g/W_c = 0.1$) fin tip gap. Therefore, the rectangular fin heat sink does not need to be fully shrouded in the case of the vertical fin tip gap. The horizontal fins with a small fin tip gap ($H_g/W_c = 0.4$) should be considered in heat sink design because they play an important role in the improvement of heat sink thermal performance.

Keywords: Microchannel heat sink; Fin tip gap; Heat transfer, Electronic cooling.

ELEKTRONİK SOĞUTMADA YATAY/DÜŞEY KANATÇIK TEPE AÇIKLIĞININ MİKROKANAL ISI KUYUSU PERFORMANSINA ETKİLERİ

Özet: Bu çalışmada, yatay ve düşey kanatçık tepe açıklığının mikrokanal ısı kuyusu performansına etkileri incelenmiştir. Üç farklı geometride (dikdörtgen, üçgen ve yamuk) mikrokanal kanatçığı üç-boyutlu olarak, farklı düşey tepe açıklıklarında tasarlanmıştır. Mikrokanal ısı kuyusu performansını simüle etmek için, sonlu hacim metodu kullanılmıştır. Çözüm, Gambit 2.3.26/FLUENT 6.3.26 yazılımı kullanılarak elde edilmiştir. Küçük düşey kanatçık ($V_g/W_c < 0.8$) tepe açıklıklarında, dikdörtgen kanatçıklı ısı kuyusu ısı direncinde küçük azalma olmakta ve $V_g/W_c = 0.8$ 'da minimum ısı direnci oluşmaktadır. Buna karşılık, kanatçıklar yamuk olduğunda, küçük kanatçık tepe açıklıklarında ($V_g/W_c \leq 0.4$) ısı direnci sabit kalmaktadır. Ancak, açıklık $V_g/W_c > 0.4$ olduğunda, ısı direnci önemli ölçüde artmaktadır. Üçgen kanatçıklı ısı kuyusu ısı direnci, bütün düşey kanatçık tepe açıklığı aralıklarında sürekli artmaktadır. Düşey kanatçık tepe açıklığının küçük olması, ısı kuyusunun performansında herhangi bir düşmeye sebep olmamaktadır, aksine özellikle dikdörtgen kanatçıklı ısı kuyularında performans artışı sağlamaktadır. Her bir düşey kanatçığın iki yüzeyine yatay kanatçıklar yerleştirilerek, dikdörtgen kanatçıklı ısı kuyusu performansına yatay kanatçık tepe açıklığının etkisi analiz edilmiştir. Optimum yatay kanatçık tepe açıklığında ($H_g/W_c = 0.1$), ısı kuyusu ısı direncinin önemli ölçüde düştüğü görülmüştür. Bu nedenle, düşey kanatçık tepe açıklığı durumunda, dikdörtgen kanatçıklı ısı kuyusunun tamamen gizlenmesine gerek yoktur. Yatay kanatçık tepe açıklığının küçük olması, ısı kuyusunun performansının artmasında önemli rol oynadığı için, yatay kanatçık tepe açıklığı küçük ($H_g/W_c = 0.4$), ısı kuyusu tasarımı tercih edilmelidir.

Anahtar Kelimeler: Mikrokanal ısı kuyusu, Kanatçık ucu açıklığı, Isı transferi, Elektronik soğutma.

INTRODUCTION

Cooling applications in electronic systems have gained significance recently. The demand for a high electronic working capacity and a reduced physical size for cooling systems has led to the increased release of heat or high temperature from electronic systems. Without

proper cooling, this high temperature will damage the electronic system due to overheating. Compared with currently available cooling technology, conventional cooling technology cannot adequately remove the high heat in certain conditions due to its limited cooling

capacity. In terms of physical size, conventional cooling technology is large, which makes it unsuitable for application systems that require a compact size. Therefore, the development of an effective cooling system with a compact size is urgently needed. In this regard, the microchannel heat sink has been considered due to its high cooling capacity.

The microchannel heat sink was first introduced by Tuckerman and Pease in 1981. They found that the microchannel heat sink can remove heat at a capacity of 7.9 MW/m^2 . Subsequently, many other researchers started to conduct detailed studies on the microchannel heat sink. Based on the literature review of Steinke and Kandlikar (2006) and Kandlikar (2006), the conventional theory of Navier–Stokes and Poiseuille flow could be applied to the single phase of fluid flow in microchannels. Sara *et al.* (2009) also found that the friction factor from their experimental result agrees well with classical Poiseuille flow theory. The experimental results of Harms *et al.* (1999) on developing flow in microchannels indicated that the local Nusselt number agrees with classical developing channel flow theory. In the study of Garimella and Singal (2004), the fluid flow and heat transfer in microchannels were examined. Pumping requirements and the suitable mechanisms for pumping the coolant through microchannels were also identified. Experimentally, they found that conventional correlations are sufficient to predict the thermal behavior of single-phase fluid flow in rectangular microchannels. Agarwal *et al.* (2010) also reported a similar observation in their study of rectangular minichannels. In the work of Garcia-Hernando *et al.* (2009), microchannels of $100 \mu\text{m} \times 100 \mu\text{m}$ and $200 \mu\text{m} \times 200 \mu\text{m}$ square cross sections were designed and tested, and they concluded that their experimental results agree well with classical viscous flow and heat transfer theory. Other researchers (Park and Punch, 2008; Barlay Ergu *et al.*, 2009; Xie *et al.*, 2009; Lee *et al.*, 2005) also made the same observation and claimed that classical theory remains applicable to fluid flow in microchannels in terms of hydrodynamic and thermal performance. Other than the verification of the applicability of classical theory to fluid flow in microchannels, various types of microchannel configurations have also been examined to investigate cooling effectiveness. An example is the work of Chen *et al.* (2009), which involved rectangular, triangular, and trapezoidal microchannels.

Jung *et al.* (2004) studied the effect of the vertical fin tip gap on microchannel heat sink performance. The effect was investigated under constant pumping power within a specific domain of a single fin and a single channel in the microchannel heat sink; the fin tip gap was considered within the channel width. Jung *et al.* (2004) found that thermal resistance could be reduced gradually by increasing the fin tip gap in a small amount and that the thermal resistance is at its minimum at the optimum vertical fin tip gap. Other researchers also conducted studies on the effect of a vertical fin tip gap larger than the channel width with air as the coolant and

with the conventional heat sink size. Various fin configurations such as the rectangular fin (Coetzer and Visser, 2003; Sata *et al.*, 1997; Li *et al.*, 2009; Elshafei, 2007), circular pin fin (Khan and Yovanovich, 2007; Moores *et al.*, 2009; Naphon and Sookkasem, 2007), and square pin fin (Dogruoz *et al.*, 2006; Jeng, 2008) were also analyzed.

Although the effect of the fin tip gap has been examined by a number of researchers, a few areas of improvement have yet to be explored. A number of approaches have been attempted to improve the heat sink, in which the further study of the effect of the vertical fin tip gap is considered significant. The entire microchannel heat sink structure and the fluid flow domain inside the heat sink, which were not studied previously by Jung *et al.* (2004), should be considered (as shown in Figure 1). The analysis of microchannel heat sink performance under a constant volume flow rate different from that in the work of Jung *et al.* is also important. The purpose of these considerations is to investigate their effects on the vertical fin tip gap compared with the results of Jung *et al.*'s work (2004). The effect of the vertical fin tip gap for various fin configurations (rectangular, triangular, and trapezoidal fin configurations, as shown in Figures 2(b), 2(d), and 2(f), respectively) has been investigated and designed in three-dimensional models. An analysis of the effect of the horizontal fin tip gap with the introduction of a horizontal fin on both sides of each vertical fin (as shown in Figure 3) is also conducted in this paper. The limit range of the vertical and the horizontal fin tip gaps is considered within the channel width. Conventional governing equations, namely, the continuity equation, the Navier–Stokes equation, and the energy equation, were solved to simulate heat sink performance.

METHODOLOGY

Microchannel Heat Sink Geometrical Configuration

Figures 1 and 2 show the geometrical dimensions of the microchannel heat sink and the various fin configurations, respectively. The dimension of the microchannel heat sink is 16.00 mm (length, L) \times 7.0809 mm (width, W) \times 0.50 mm (height, H). Three types of fin configurations have been analyzed in this study, namely, rectangular, triangular, and trapezoidal fins. The physical dimensions of the microchannel heat sink are the same for all fin configurations, except for the fin dimensions. For the comparison of heat sink performance among the three fin configurations, the same hydraulic diameter for each microchannel configuration is set at the initial stage without the fin tip gap, as indicated in Figures 2(a), 2(c), and 2(e). Then the fin height of each fin configuration is reduced gradually to analyze the effect of the vertical fin tip gap on the heat sink hydrodynamic and thermal performance. The height of each fin configuration is reduced within the channel width and is denoted as V_g , as shown in Figures 2(b), 2(d), and 2(f).

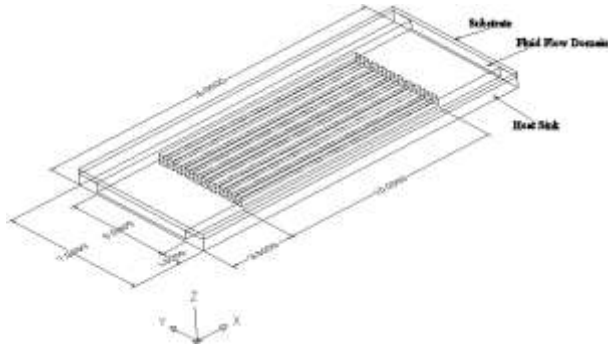


Figure 1. Geometrical configuration dimensions of microchannel heat sink (all dimensions in mm).

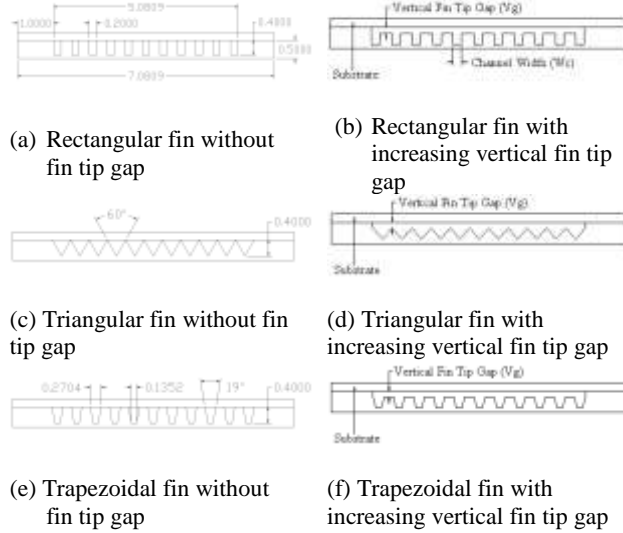


Figure 2. Dimensions of cross sectional microchannel heat sink (all dimensions in mm) and schematic diagram of various fin configurations without and with vertical fin tip gap.

After the optimum vertical fin tip gap has been determined (with the lowest total thermal resistance), the horizontal fin is introduced at both sides of each vertical fin, as shown in Figure 3(a). Further analysis is conducted on the effect of the horizontal fin tip gap, H_g . The horizontal fin tip gap is also analyzed within the channel width, in which it is reduced until both ends of the horizontal fins are fully joined, as shown in Figure 3(b). All these microchannel heat sinks are attached directly to a CPU microprocessor chip from which the heat flux is generated and then transferred to the heat sink base.

Computational Model

The effect of the vertical and the horizontal fin tip gaps has been studied based on the following assumptions:

- Fluid flow and heat transfer are in a steady state condition.
- The coolant is a single-phase fluid flow.
- The flow is laminar.
- The properties of the fluid and the microchannel heat sink are constant due to minimal changes in temperature between the inlet and the outlet of the microchannel heat sink.

- Heat sink surfaces exposed to surroundings are assumed as adiabatic, except for the heat sink base surface where heat flux is applied.

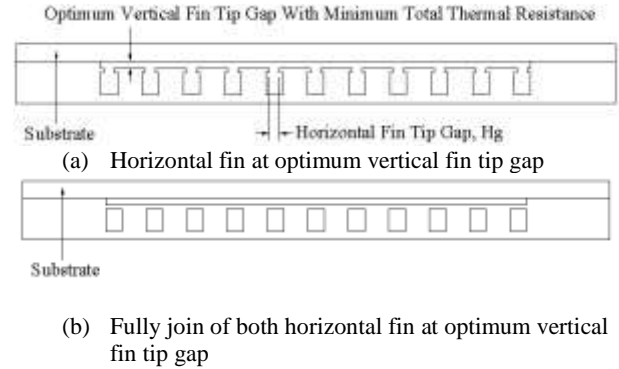


Figure 3. Horizontal fin and fully join of both horizontal fins at optimum vertical fin tip gap.

Finite volume method (FVM) is used to solve the following governing equations in order to simulate the hydrodynamic and heat transfer of fluid flow in the microchannel heat sink. The simulation is conducted using Gambit 2.3.26/FLUENT 6.3.26 software.

Continuity equation:

$$\frac{\partial u}{\partial x} + \frac{\partial v}{\partial y} + \frac{\partial w}{\partial z} = 0 \quad (1)$$

Momentum equation:

$$u \frac{\partial u}{\partial x} + v \frac{\partial u}{\partial y} + w \frac{\partial u}{\partial z} = -\frac{1}{\rho_f} \frac{\partial P}{\partial x} + \frac{\mu}{\rho_f} \left(\frac{\partial^2 u}{\partial x^2} + \frac{\partial^2 u}{\partial y^2} + \frac{\partial^2 u}{\partial z^2} \right) \quad (2a)$$

$$u \frac{\partial v}{\partial x} + v \frac{\partial v}{\partial y} + w \frac{\partial v}{\partial z} = -\frac{1}{\rho_f} \frac{\partial P}{\partial y} + \frac{\mu}{\rho_f} \left(\frac{\partial^2 v}{\partial x^2} + \frac{\partial^2 v}{\partial y^2} + \frac{\partial^2 v}{\partial z^2} \right) \quad (2b)$$

$$u \frac{\partial w}{\partial x} + v \frac{\partial w}{\partial y} + w \frac{\partial w}{\partial z} = -\frac{1}{\rho_f} \frac{\partial P}{\partial z} + \frac{\mu}{\rho_f} \left(\frac{\partial^2 w}{\partial x^2} + \frac{\partial^2 w}{\partial y^2} + \frac{\partial^2 w}{\partial z^2} \right) \quad (2c)$$

Fluid flow - Energy equation:

$$u \frac{\partial T}{\partial x} + v \frac{\partial T}{\partial y} + w \frac{\partial T}{\partial z} = \frac{k_f}{\rho_f c_{pf}} \left(\frac{\partial^2 T}{\partial x^2} + \frac{\partial^2 T}{\partial y^2} + \frac{\partial^2 T}{\partial z^2} \right) \quad (3)$$

As reported by Koo and Kleinstreuer (2004), the effect of viscous dissipation would significantly affect fluid with low specific heat capacity and high viscosity, as well as fluid flow within the channel with a hydraulic diameter $< 50 \mu\text{m}$. The hydraulic diameter of the microchannel is $267 \mu\text{m}$, and the working fluid (water) is low-viscosity fluid with high specific heat capacity. Thus, the effect of viscous dissipation on the working fluid can be neglected. Furthermore, the Brinkman number for the fluid flow (under all hydrodynamic and thermal conditions which have been considered in this study) shows a substantially small value, which is on average 7.0198×10^{-5} and is very far from unity. As a result, the effect of viscous dissipation is not vital in this study and can be neglected.

Solid – Conduction equation:

$$\frac{\partial^2 T}{\partial x^2} + \frac{\partial^2 T}{\partial y^2} + \frac{\partial^2 T}{\partial z^2} = 0 \quad (4)$$

Based on the assumptions that have been made above, the boundary conditions are applied as follows:

At inlet of microchannel heat sink:
 $u = u_{in}; T = T_{in}$ (5a)

Interface between solid and fluid:
 $u = v = w = 0 \text{ ms}^{-1}; T = T_s;$
 $-k_s \frac{\partial T_s}{\partial n} = -k_f \frac{\partial T}{\partial n}$ (5b)

At the heat sink base:
 $q'' = -k_s \frac{\partial T_s}{\partial n}$ (5c)

At outlet of microchannel heat sink:
 $P = P_{out};$
 $\frac{\partial T}{\partial n} = 0$ (5d)

Water is used as coolant, and the heat sink material is considered as aluminum. The properties of the coolant and the heat sink material are summarized in Table 1. The coolant temperature at the inlet is set as 300 K. The performance of the microchannel heat sink is analyzed in the range of 0.00 mm to 0.20 mm (within the channel width) for the vertical fin tip gap. A similar range is also used for the horizontal fin tip gap. A heat flux of 300,000 W/m² is considered generated from the microchannel heat sink base. The subscript *f* that appears in Equations (2a), (2b), (2c), (3), and (5b) is denoted as a fluid for the coolant, whereas *s* that appears in Equations (5b) and (5c) is denoted as a solid for the heat sink.

Table 1. Properties of coolant (at 300K) and heat sink (Holman, 1992)

Parameters	Domain Substance	
	Coolant	Heat Sink
Material	Water	Aluminum
Density (kg/m ³)	995.8	2707
Specific Heat (J/kg.K)	4179	896
Conductivity (W/m.K)	0.614	204
Dynamic Viscosity (Ns/m ²)	0.00086	-

In FVM, SIMPLE algorithm is used to solve the pressure fields. The pressure term is discretized by standard discretization, and momentum and energy terms are discretized by second-order upwind scheme. The simulation takes approximately 10 hours in Intel (R) Xeon (R) CPU W3520 processor of 2.67 GHz with 12.0 GB RAM.

Grid Independency Test

Three grid sizes have been studied in the grid independency test, namely, 4.99 x 10⁵, 11.30 x 10⁵, and 21.49 x 10⁵ grids, to ensure that the numerical results

are independent of the grid size. The rectangular fin heat sink without any fin tip gap is considered for the test. Figure 4 and Figure 5 show the comparison of velocity and temperature, respectively, along the centerline of the sixth channel among various grid sizes. The figures show that the grid sizes of 11.30 x 10⁵ and 21.49 x 10⁵ are almost close to each other, with a less than 1.0% difference between them. Hence, the grid size of 11.30 x 10⁵ is chosen and applied throughout the numerical calculation due to the small computing time and memory usage involved.

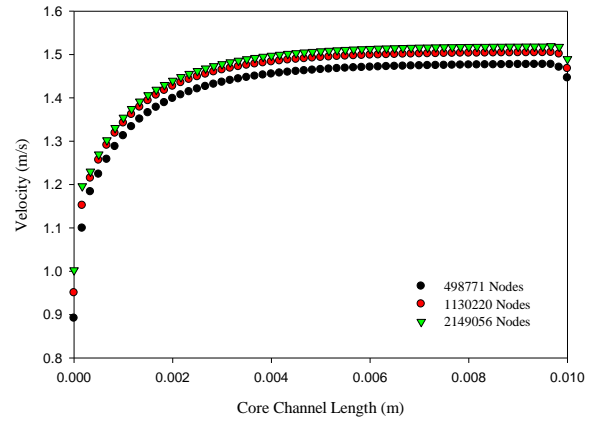


Figure 4. Comparison of fluid flow velocity along center line of 6th channel among various grid sizes in rectangular fin heat sink (without any fin tip gap).

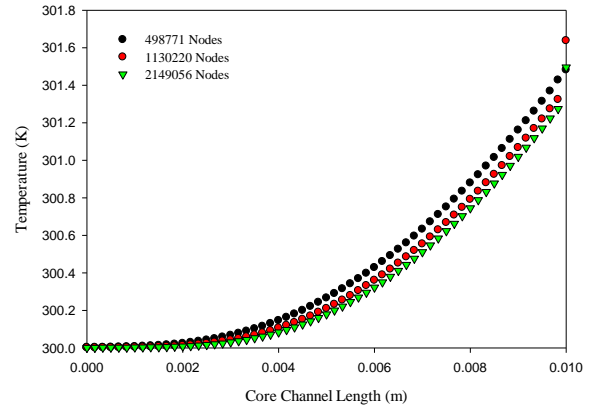


Figure 5. Comparison of fluid flow temperature along center line of 6th channel among various grid sizes in rectangular fin heat sink (without any fin tip gap).

Model Validation

The simulation result of the rectangular fin microchannel heat sink has been verified with theoretical correlations, as done by Kandlikar [3]. Two main parameters are considered for verification: pressure drop and Nusselt number. The verification is made within Re numbers 239 and 982, and the heat flux is considered as 500,000 W/m² generated from the heat sink base.

Figure 6 shows that the average pressure drop agrees well with the theoretical correlation.

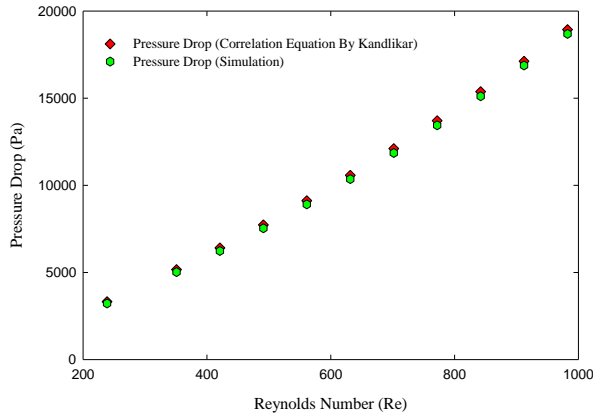


Figure 6. Pressure drop comparison between simulation and theoretical correlation results as function of Re number in rectangular fin microchannel heat sink (without fin tip gap).

The theoretical correlation of the pressure drop is calculated with the following equations (Kandlikar, 2006):

$$\Delta P = \frac{2f_{app}\rho u_m^2 x}{D_h} \quad (6)$$

where

$$\text{Apparent friction factor, } f_{app} = \left(\frac{1}{Re}\right) \left(\frac{142.05+1481(x^+)^{0.5}+13177(x^+)}{1-5.4166(x^+)^{0.5}+1067.8(x^+)-108.52(x^+)^{1.5}}\right) \quad (7)$$

$$\text{Non-dimensionalized length, } x^+ = \frac{\left(\frac{x}{D_h}\right)}{Re} \quad (8)$$

D_h is the hydraulic diameter, x is the length from the channel entrance, and u_m is the mean fluid flow velocity.

Similarly, in Figure 7, the simulated average Nusselt number has also been compared with the theoretical correlation. The simulated Nusselt number agrees with the theoretical correlation and shows the same trend along the various Re numbers.

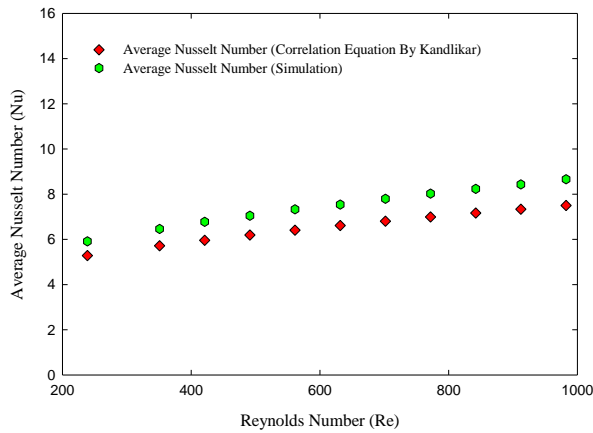


Figure 7. Nusselt number comparison between simulation and theoretical correlation results as function of Re number in rectangular fin microchannel heat sink (without fin tip gap) with heat flux of 500000W/m² generated to heat sink base. The theoretical correlation of the Nusselt number is calculated according to Equation [3], as follows:

$$Nu_{x,3}(x^*, \alpha_c) = Nu_{x,4}(x^*, \alpha_c) \frac{Nu_{fd,3}(x^*=x_{fd}^*, \alpha_c)}{Nu_{fd,4}(x^*=x_{fd}^*, \alpha_c)} \quad (9)$$

where

$$Nu_{x,4}(x^*, \alpha_c) = \frac{28.315+27038(x^*)+1783300(x^*)^2}{1+3049(x^*)+472520(x^*)^2-35714(x^*)^3} \quad (10)$$

$$Nu_{fd,3}(x^* = x_{fd}^*, \alpha_c) = \frac{8.2321+1.2771(\alpha_c)+2.2389(\alpha_c)^2}{1+2.0263(\alpha_c)+0.29805(\alpha_c)^2+0.0065322(\alpha_c)^3} \quad (11)$$

$$Nu_{fd,4}(x^* = x_{fd}^*, \alpha_c) = \frac{8.2313-2.295(\alpha_c)+7.928(\alpha_c)^2}{1+1.9349(\alpha_c)+0.92381(\alpha_c)^2+0.0033937(\alpha_c)^3} \quad (12)$$

$$\text{Non-dimensionalized length, } x^* = \frac{\left(\frac{x}{D_h}\right)}{Re \cdot Pr} \quad (13)$$

α_c is channel aspect ratio and Pr is Prantl number.

Thus, the positive results of verification for both parameters show that the predictions made by the Gambit 2.3.26/FLUENT software are reliable and can simulate the hydrodynamic and thermal performance of the microchannel heat sink.

RESULT AND DISCUSSION

Effect of Vertical Fin Tip Gap In Various Fin Configurations

Hydrodynamic performance

Figure 8 shows that the pressure drop in the microchannel heat sink decreases with an increase in the vertical fin tip gap V_g at a constant volume flow rate for each type of fin configuration. The reduction in pressure drop is due to the lower flow resistance as the tip gap increases. The triangular fin heat sink has the lowest pressure drop. As shown in Figure 9, the triangular fin heat sink provides the lowest surface area compared with the trapezoidal and rectangular fin heat sinks. As a result, a low pressure force is required to overcome the frictional force due to the shear force on the heat sink surface. As seen in Equation (14) (Xie *et al.*, 2009; Shokouhmand *et al.*, 2008), the pumping power is proportionally related to the pressure drop:

$$\text{Pumping power, } P_{\text{pumping}} = \Delta P \cdot Q \quad (14)$$

where ΔP is pressure drop and Q is volume flow rate.

Pumping power is a parameter that is as significant as the pressure drop. Hence, the lowest pumping power is required to drive the coolant flow through the triangular microchannels. However, the rectangular fin heat sink shows the highest pressure drop due to the high heat sink surface area (as shown in Figure 9 and Figure 10). This high heat sink surface area requires a high pressure force to overcome the frictional force on the surface

area and results in a high pumping power requirement to drive the coolant flow through the rectangular microchannels. Consequently, the triangular fin heat sink shows the best hydrodynamic performance compared with the trapezoidal and rectangular heat sinks. Although the triangular fin heat sink has shown good hydrodynamic performance, the thermal performance of the heat sink needs to be analyzed further before a conclusion can be reached.

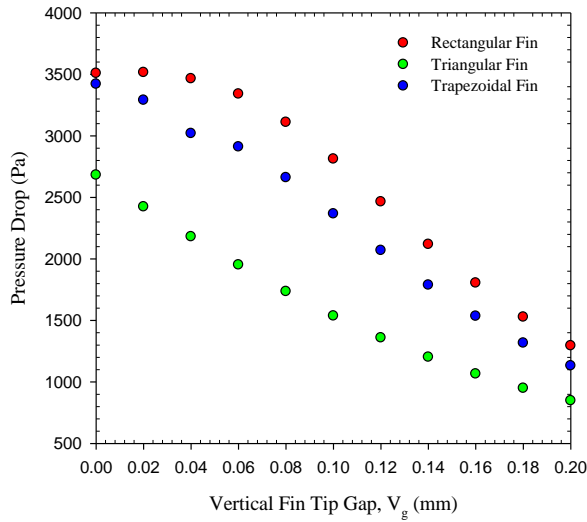


Figure 8. Comparison of pressure drop as function of vertical fin tip gap, among various fin configurations of microchannel heat sinks at volume flow rate of $6.8 \times 10^{-7} \text{ m}^3/\text{s}$.

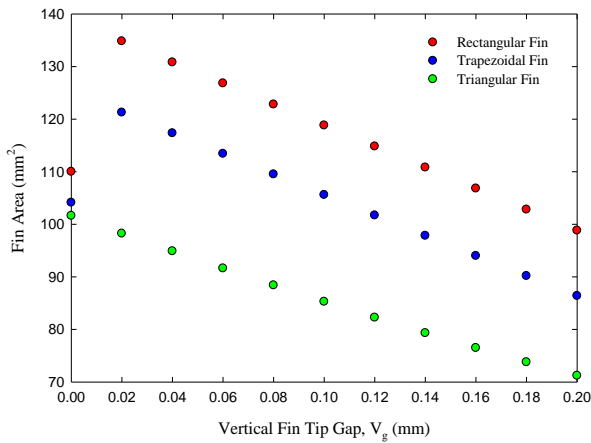


Figure 9. Fin area as function of vertical fin tip gap for various fin configurations of microchannel heat sinks.

Thermal performance

In thermal analysis, the thermal performance of the microchannel heat sink can be conveniently explained in terms of total thermal resistance. Three types of thermal resistance are considered: thermal convective resistance, thermal capacity resistance, and thermal conductivity resistance. Hence, the total thermal resistance can be determined according to Equation (15) (Xie *et al.*, 2009), as follows:

$$R_{th,total} = \frac{1}{\bar{h}A_{sf}} + \frac{1}{\dot{m}c_p} + \frac{1}{\left(\frac{k_s A_b}{H_b}\right)} \quad (15)$$

where effective fin convective area,

$$A_{sf} = nW_c L + 2n\eta H_c L \quad (16)$$

\bar{h} is the average convective heat transfer coefficient, H_b is the heat sink base thickness, W_c is the channel width, H_c is the fin height, n is the number of channels, η is the fin efficiency, and A_b is the heated heat sink base surface.

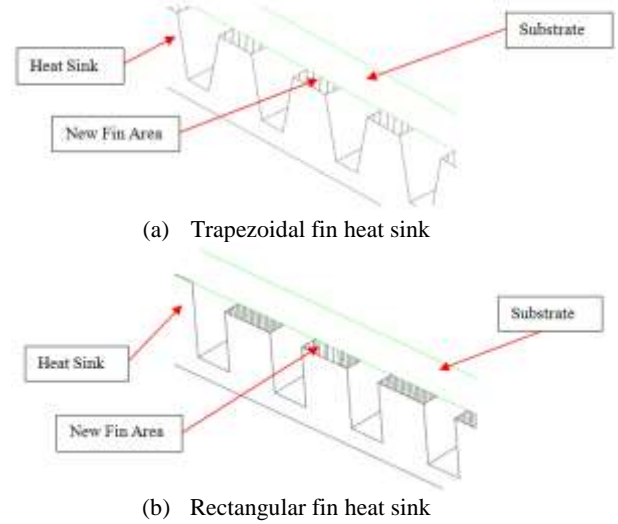


Figure 10. Introduction of new fin area as the vertical fin tip gap is introduced.

From Figure 11, the triangular fin heat sink shows a continuous increase in total thermal resistance with an increase in the vertical fin tip gap. This increase is due to the continuous decrease in the fin surface area, A_{sf} , as shown in Figure 9. With this decrease in fin area, lesser heat can be convectively transferred into the fluid flow. Moreover, the velocity distribution of the fluid flow in the core channel also affects the convective heat transfer. As indicated in Figure 12(a), the profile of velocity distribution in the triangular channel is not symmetrical in all ranges of vertical gaps. The velocity at the lower part of the core channel is low, and this causes low convective heat transfer. As a result, the total thermal resistance of the triangular fin heat sink becomes higher compared with those of the trapezoidal and rectangular fin heat sinks.

With regard to the trapezoidal fin heat sink, a constant trend can be seen at the vertical gap $<0.06 \text{ mm}$, as shown in Figure 11. As the vertical gap increases within the range, the fluid flow velocity in the core channel is slightly decreased (as indicated in Figure 12(b)), and the convective heat transfer is slightly decreased. However, with the increment in fin area from the top surface of the trapezoidal fins (as indicated in Figure 9 and Figure 10(a)), the additional fin area allows good contact with the fluid flow for convective heat transfer. Hence, this additional area will compensate for the minimal decrease in convective heat transfer due to the decrease

in fluid flow velocity. The total thermal resistance is almost constant at the vertical gap <0.06 mm. As the vertical gap increases >0.04 mm, the total thermal resistance also increases at a high rate. This increase is attributed to the decrease in fin area as well as the evident decrease in fluid flow velocity in the core channel, as shown in Figure 9 and Figure 12(b), respectively. From Figure 12(b), the fluid flow velocity distribution in the core channels is not symmetrical within all ranges of vertical gaps. From the observation on the lower part of the fluid flow velocity distribution, the low fluid flow velocity causes low convective heat transfer from the lower part of the core channel. As a result, the total thermal resistance of the trapezoidal fin heat sink is higher than the thermal resistance of the rectangular fin heat sink.

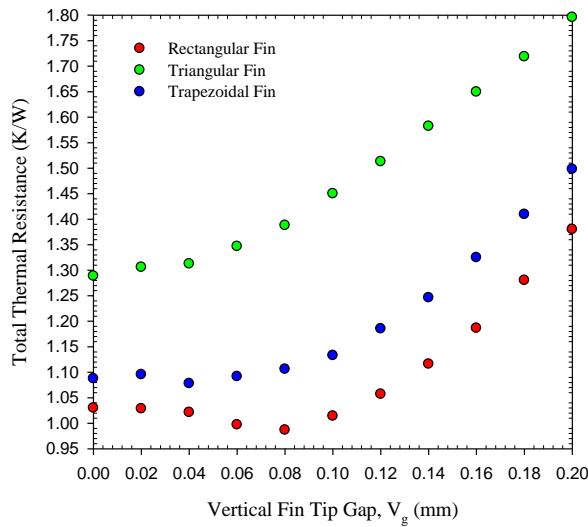
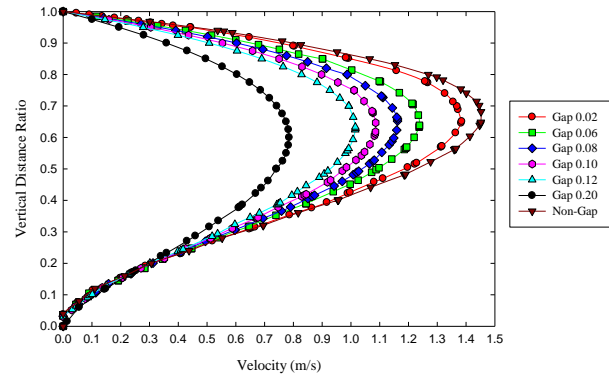


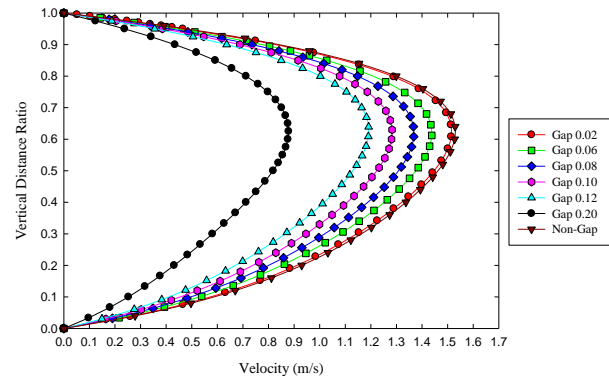
Figure 11. Comparison of total thermal resistance as function of vertical fin tip gap, among various fin configurations of microchannel heat sinks at volume flow rate of $6.8 \times 10^{-7} \text{ m}^3/\text{s}$ and heat flux of 300000 W/m^2 .

With regard to the rectangular fin heat sink, the constant trend of thermal resistance can also be seen at a vertical gap <0.04 mm, as shown in Figure 11. This phenomenon can be explained similarly as in the case of the trapezoidal fin heat sink, in which the increment in the fin area from the fin tip is also present, as shown in Figure 9 and Figure 10(b). Within the vertical gap $0.04 \text{ mm} < V_g < 0.08$ mm, the heat sink performance shows a decreasing total thermal resistance and achieves the lowest total thermal resistance at a V_g of 0.08 mm. The performance shows a 4.18% reduction compared with the thermal resistance of the non-fin tip gap heat sink. This achievement of the lowest total thermal resistance can be explained as follows. As V_g increases from 0.04 mm to 0.08 mm, although the fluid flow velocity (in the core channel) decreases, the symmetrical fluid flow velocity distribution is still effective in the convective removal of heat. Furthermore, the fin area is larger compared with that in the non-vertical gap case. Hence, the total thermal resistance decreases within this range. With the further analysis of a $V_g > 0.08$ mm, the total thermal resistance

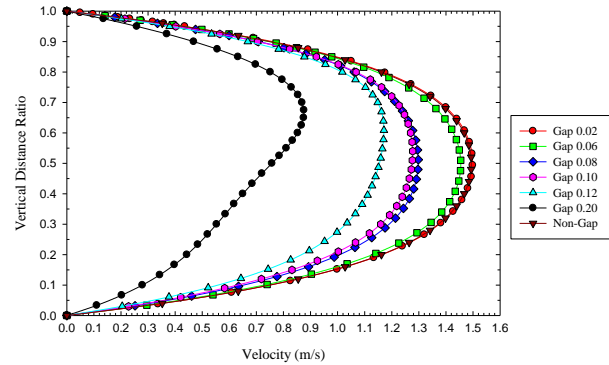
increases continuously at a high rate due to the unsymmetrical fluid flow velocity distribution, as shown in Figure 12(c). At a V_g of 0.10 mm, the peak fluid flow velocity begins to shift upward, and the velocity at the lower part of the core channel becomes lower compared with that in the upper part of the core channel. As V_g keeps increasing, the fluid flow velocity in the lower part of the core channel becomes further reduced, as can be seen in the vertical gaps of 0.12 mm and 0.20 mm. Consequently, the convective heat transfer becomes low under a low fluid flow velocity. Simultaneously, the fin area also decreases as V_g increases (as shown in Figure 9), which causes the convective heat transfer to become low as well.



(a) Triangular fin heat sink



(b) Trapezoidal fin heat sink



(c) Rectangular fin heat sink

Figure 12. Velocity distribution at different vertical fin tip gaps in 6th core channel of triangular-, trapezoidal- and rectangular- fins of microchannel heat sinks at volume flow rate of $6.8 \times 10^{-7} \text{ m}^3/\text{s}$.

The contour of temperature distribution on the heat sink base is shown in Figure 13 to attain a clear view of the heat sink thermal performance among various fin configurations. As can be seen from Figure 13(a), the high-temperature area on the triangular fin heat sink base is the widest compared with the rectangular and trapezoidal fin heat sinks. This wide high-temperature area is due to the high total thermal resistance. From Figure 13(b), the trapezoidal fin heat sink shows a wider low-temperature area than that of the triangular fin heat sink. In the case of the rectangular fin heat sink, an even wider low-temperature area can be seen, as illustrated in Figure 13(c). This case can be attributed to the low total thermal resistance that enables the easy transfer of heat from the heat sink into the fluid flow.

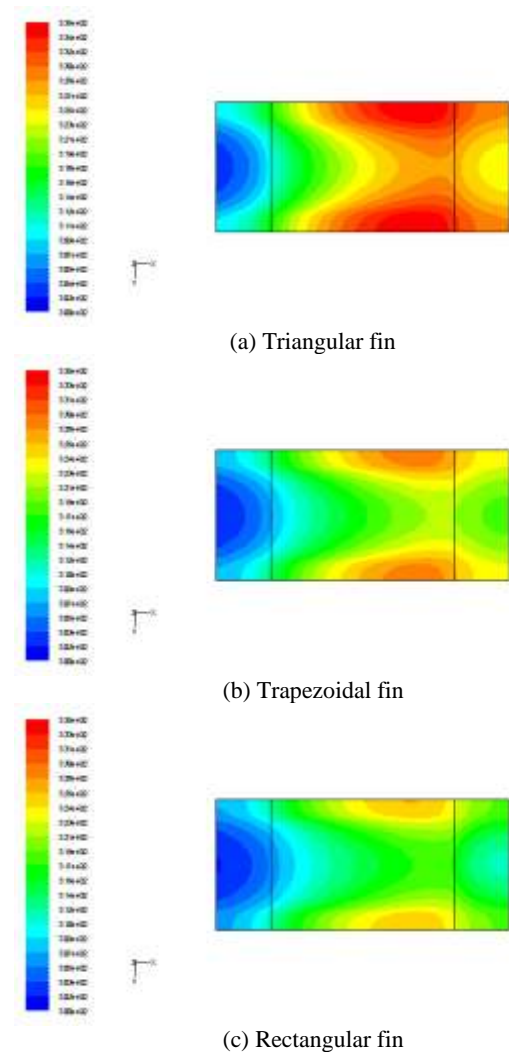


Figure 13. Temperature contour of heat sink base among various fin configurations of microchannel heat sink at vertical fin tip gap of 0.08mm, volume flow rate of $6.8 \times 10^{-7} \text{ m}^3/\text{s}$ and heat flux of 300000 W/m^2 .

As a common engineering practice in industries, dimensional tolerance in producing any heat sink is required due to uncertainty in the production process. As a result, the allowable dimensional tolerance of the vertical fin tip gap for the rectangular fin can be assigned to the ratio V_g/W_c (ratio of the vertical fin tip gap to the core channel width) of 0.4. Within the range

of $V_g/W_c \leq 0.4$, the rectangular fin heat sink can still execute effective heat removal without a deterioration in its thermal performance. This effective heat removal is the advantage of using the rectangular fin configuration in heat sink design. Although the trapezoidal fin heat sink has shown an almost constant total thermal resistance within the range of $V_g/W_b \leq 0.3$ (the vertical fin tip gap to the core channel bottom width), it can still be considered as an alternative option, although its thermal resistance is slightly higher than that of the rectangular fin (on average 7% higher). The triangular fin heat sink has shown good hydrodynamic performance but poor thermal performance. As a result, the existence of a small limited range of the vertical gap ($V_g/W_c \leq 0.4$) would not worsen the thermal performance as in the case of the rectangular fin heat sink; instead, it will reduce thermal resistance. Hence, the rectangular fin configuration is the best option for heat sink design. Furthermore, such configuration is a common fin design in engineering applications, as it affords ease in fabrication. As the rectangular fin can maintain/provide good thermal performance with the existence of the vertical fin tip gap within a small range, the rectangular fin is selected for further analysis in the following.

Effect of Vertical Fin Tip Gap In Various Volume Flow Rate Conditions

Hydrodynamic performance

As shown in Figure 14, both cases of the rectangular fin heat sink with ($V_g/W_c=0.4$) and without ($V_g/W_c=0.0$) a vertical fin tip gap show an incremental pressure drop as the volume flow rate increases. Along with the increment of volume flow rate, the difference in pressure drop between both cases increases. This difference shows that the heat sink with a vertical gap can work even better than that without a vertical gap in terms of hydrodynamic performance at a high volume flow rate. As a result, the existence of a vertical gap would not worsen the hydrodynamic performance of the heat sink; instead, it would reduce flow resistance.

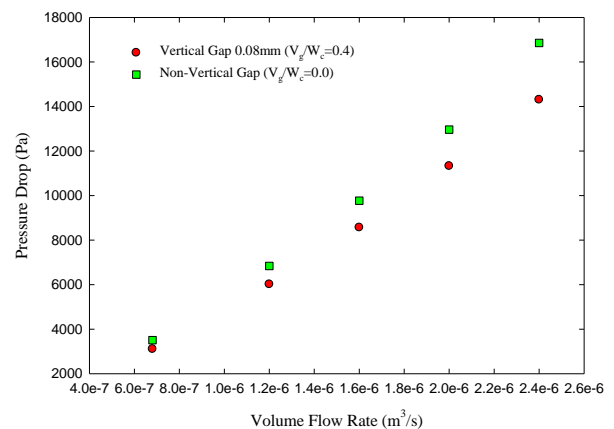


Figure 14. Comparison of pressure drop as function of volume flow rate between non- and with vertical- fin tip gap.

Thermal performance

As depicted in Figure 15, the total thermal resistance for both cases of the rectangular fin heat sink with and without a vertical fin tip gap shows a decrease as the volume flow rate increases. This phenomenon indicates that the existence of the small vertical fin tip gap does not cause the deterioration of heat sink thermal performance within the range of $V_g/W_c \leq 0.4$. Instead, it enables the heat sink to maintain or even produce a better thermal performance than that of the non-vertical gap heat sink. The microchannel heat sink does not need to be fully shrouded to achieve the maximum thermal performance, as mentioned by Jung et al. [14]. As a result, the small vertical fin tip gap is allowable but limited to the ratio V_g/W_c of 0.4 to ensure the good thermal performance of the heat sink.

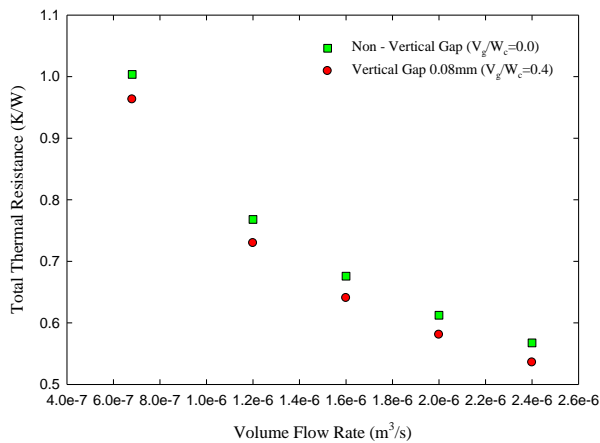


Figure 15. Comparison of total thermal resistance as function of volume flow rate between non- and with vertical- fin tip gap at heat flux of 300000 W/m^2 .

Effect of the Horizontal Fin Tip Gap

Hydrodynamic performance

After the optimum/allowable vertical fin tip gap has been determined, the horizontal fins are introduced at both sides of each vertical rectangular fin tip, as shown in Figure 16. The horizontal fin tip gap can be conveniently expressed in terms of a dimensionless parameter as a ratio of the horizontal fin tip gap to the channel width, H_g/W_c . As shown in Figure 17, the pressure drop increases slightly in the range $H_g/W_c \leq 0.1$. This drop is due to the higher pressure force required to overcome the frictional force with the shear force from the additional fin surface area at $H_g/W_c=0.1$ (as shown in Figs. 16 and 18). However, the pressure drop decreases at $H_g/W_c > 0.1$ due to the decrease in fin surface area, which in turn causes the decreasing force requirement to overcome the frictional force on the fin surface. Hence, a lower pumping power is required to drive the coolant at a larger H_g/W_c .

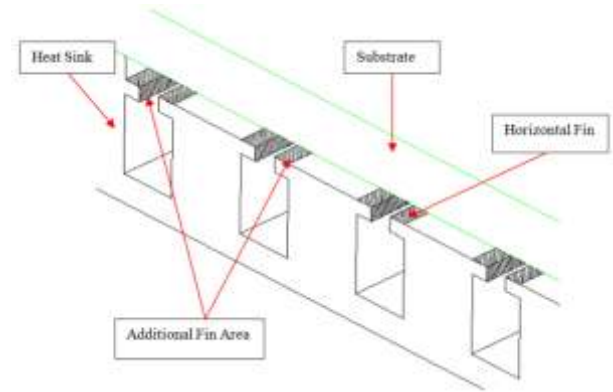


Figure 16. Introduction of new fin area as the horizontal fin is introduced.

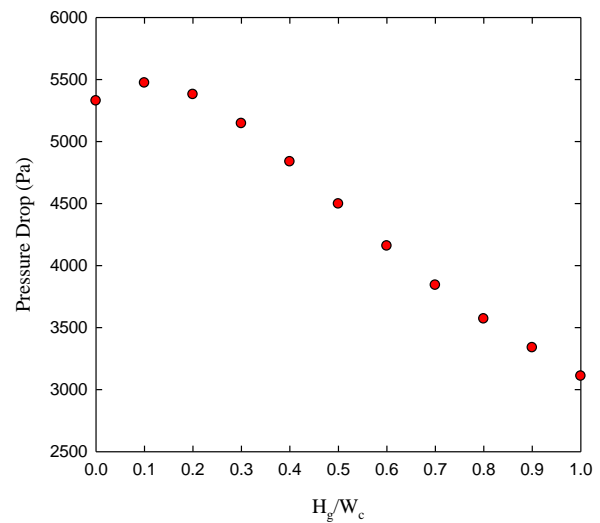


Figure 17. Pressure drop as function of horizontal fin tip gap in microchannel heat sink at optimum vertical fin tip gap condition at volume flow rate of $6.8 \times 10^{-7} \text{ m}^3/\text{s}$.

Thermal performance

The thermal performance of the rectangular fin heat sink with a horizontal fin tip gap is analyzed, as depicted in Figure 18. As shown in the figure, the total thermal resistance decreases at $H_g/W_c \leq 0.1$. The occurrence of this phenomenon is due to the additional fin area at $H_g/W_c=0.1$. Hence, more contact area is allowed between the fin surface and the fluid flow, and more heat can be dissipated into the fluid flow. The optimum gap provides the smallest total thermal resistance. As the horizontal fin tip gap increases $H_g/W_c > 0.1$, the total thermal resistance increases continuously at a high rate. This increase results from the decrement in the fin area, which consequently results in a small contact area between the fin surface and the fluid flow. Therefore, lesser heat is transferred into the fluid flow.

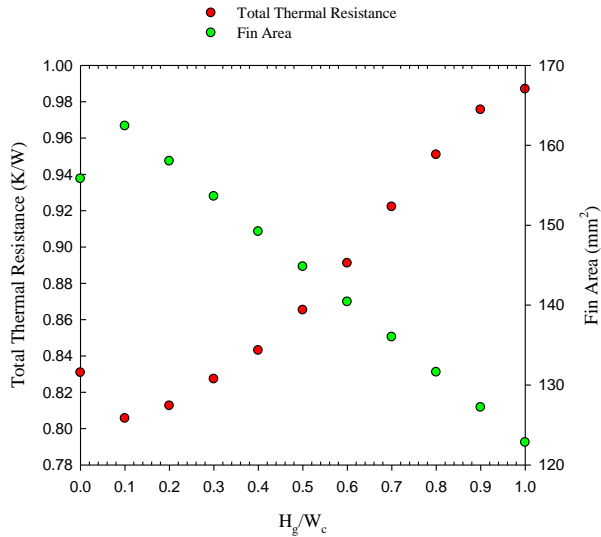


Figure 18. Total thermal resistance and fin area as function of horizontal fin tip gap in microchannel heat sink at optimum vertical fin tip gap condition at volume flow rate of $6.8 \times 10^{-7} \text{ m}^3/\text{s}$ and heat flux of 300000 W/m^2 .

The comparison of the total thermal resistance and the temperature contour of the heat sink base is summarized in Table 2 to provide a general view on the effects of vertical/horizontal fin tip gaps for the case of the rectangular fin heat sink. The summary shows that the total thermal resistance for the heat sink without any fin tip gaps is 1.0299 K/W . With the existence of the optimum vertical fin tip gap at $V_g/W_c=0.4$, the total thermal resistance is reduced to 0.9869 K/W . The improvement in thermal performance is approximately 4.18% only. With the introduction of the optimum horizontal fin tip gap at $H_g/W_c=0.1$, together with the optimum vertical fin tip gap, the heat sink thermal performance is further reduced to 0.8056 K/W . Therefore, the heat sink thermal performance is significantly improved as it becomes 21.78% lower than that of the non-fin tip gap heat sink. With consideration of the effect of the vertical fin tip gap, the existence of the horizontal fin tip gap evidently affects heat sink thermal performance.

In visualizing the effect of the vertical fin tip gap, a wider low-temperature area can be seen compared with that of the non-fin tip gap heat sink. In the case of the combination of optimum vertical–horizontal fin tip

gaps, an even wider low-temperature area can be seen. Hence, the introduction of the horizontal fin onto each vertical fin evidently improves the heat sink thermal performance as long as the vertical fin tip gap is within the range of $V_g/W_c \leq 0.4$. The horizontal fin tip gap needs to be made as close as possible to $H_g/W_c=0.1$ in order to achieve the minimum thermal resistance; this minimum thermal resistance is the main advantage of the small horizontal fin tip gap. Furthermore, the horizontal fin tip gap will not result in the deterioration of thermal performance; instead, it can help further improve heat sink thermal performance. Practically, the small horizontal fin tip gap can be considered and applied to the heat sink in order to enhance thermal performance.

Effect of Horizontal Fin Tip Gap In Various Volume Flow Rate Conditions

Hydrodynamic performance

As shown in Figure 19, the pressure drop increases as the volume flow rate increases for both cases of $H_g/W_c=0.1$ and $H_g/W_c=1.0$. Comparatively, the pressure drop for $H_g/W_c=0.1$ is higher than that for $H_g/W_c=1.0$ along various volume flow rates. The main reason is the higher fin surface area in $H_g/W_c=0.1$, which requires a higher pressure force to overcome the frictional force due to the shear force at the fin surface. Other than this, the minor loss effects of flow contraction into the horizontal fin tip gap and the expansion from the horizontal fin tip gap also contribute to the high pressure drop.

Thermal performance

As shown in Figure 20, both cases of $H_g/W_c=0.1$ and $H_g/W_c=1.0$ show a decrease in total thermal resistance with an increase in volume flow rate. The total thermal resistance for $H_g/W_c=0.1$ is lower than that for $H_g/W_c=1.0$ along various volume flow rates, and the existence of a horizontal fin tip gap would not worsen the thermal performance of the heat sink. Rather, the horizontal fin tip gap enables the heat sink to work effectively. Although the case $H_g/W_c=0.1$ has shown poor performance hydrodynamically, as seen in Figure 19, attention needs to be given to the positive thermal performance of the heat sink. However, options that depend on the type of engineering application involved

Table 2. Comparison of thermal performance between cases of non- fin tip gap, optimum vertical-fin tip gap and optimum vertical/horizontal- fin tip gaps in the rectangular fin microchannel heat sink.

	Heat sink without fin tip gap	Heat sink with optimum vertical fin tip gap	Heat sink with optimum vertical/horizontal fin tip gaps
Total Thermal Resistance (K/W)	1.0299	0.9869	0.8056
Temperature Contour of Heat Sink Base			

should be made available. For instance, if certain engineering applications require excellent computer performance alongside the ability to withstand high temperature, high thermal performance becomes the priority option to meet the requirement; at the same time, researchers also need to address the poor hydrodynamic performance that requires high pumping power in order to drive the coolant flow through the microchannel heat sink. Hence, a higher cost is incurred for this requirement. If the engineering applications involved do not require high cooling, a low thermal and high hydrodynamic performance becomes the option to meet this requirement. As a result, a lower cost is incurred for this requirement.

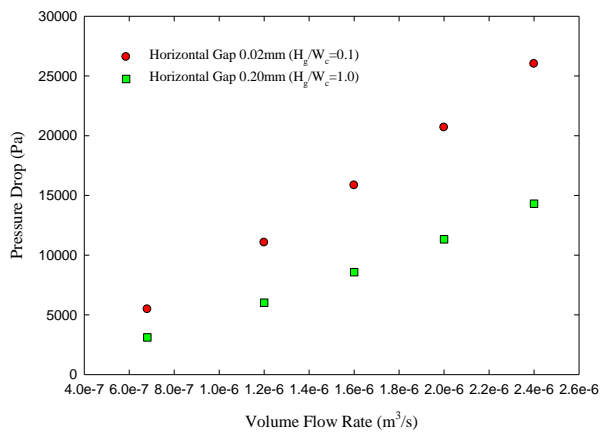


Figure 19. Comparison of pressure drop as function of volume flow rate between cases of non- and with horizontal-fin tip gap.

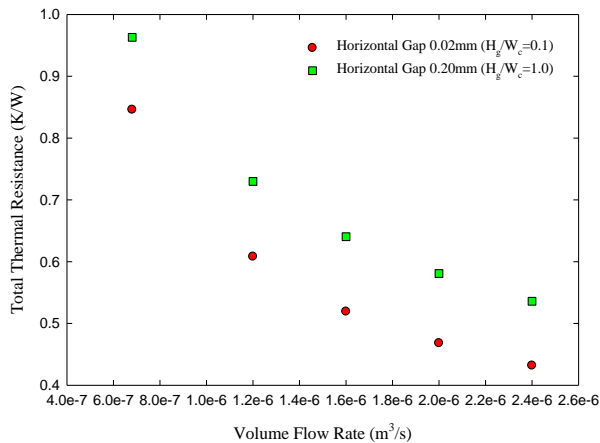


Figure 20. Comparison of total thermal resistance as function of volume flow rate between cases of non- and with horizontal-fin tip gap.

CONCLUSIONS

Among various fin configurations in all ranges of vertical fin tip gaps, the triangular fin heat sink has shown good hydrodynamic performance but is poor in thermal performance. However, for engineering applications in which low thermal performance is sufficient, the triangular fin heat sink can be an option for the cooling function requirement. The triangular fin heat sink's main advantage is its low pressure drop,

which results in a low pumping power requirement. The rectangular fin heat sink is poor in hydrodynamic performance but has good thermal performance compared with the triangular and the trapezoidal fin heat sinks. Within the vertical fin tip gap of $V_g/W_c \leq 0.4$, the heat sink can still maintain or even produce good thermal performance. Hence, the existence of the small vertical fin tip gap within such range will not affect the heat sink thermal performance, and the heat sink does not need to be fully shrouded. With the introduction of the horizontal fin on each side of each vertical fin, the thermal performance of the rectangular fin heat sink can be further increased. At the optimum horizontal fin tip gap of $H_g/W_c=0.1$, the total thermal resistance is smallest, and it is the highest thermal performance that can be achieved by the heat sink. For high cooling requirements, the rectangular fin configuration is the best choice. The horizontal fin with the optimum horizontal fin tip gap can be considered in heat sink design because it can significantly improve heat sink thermal performance.

For future research, the examination of the horizontal fin tip gap's effect can be extended by analyzing the effect of the number of the optimum horizontal fin tip gaps on several numbers of pairs of horizontal fins made along each vertical rectangular fin. Consequently, the heat sink thermal performance can be improved further to more than 21.78% reduction in thermal resistance. Research in this area can also be extended to an analysis of the thickness effect of horizontal fins, which may affect the heat sink thermal performance and the hydrodynamic performance.

REFERENCES

- Agarwal G., Moharana, M. K. and Khandekar, S., 2010, Thermo-hydrodynamics of developing flow in a rectangular mini-channel array, *20th National and 9th International ISHMT – ASME Heat and Mass Transfer Conference* DOI: 10.3850/9789810838133_351.
- Barlay Ergu, O., Sara, O. N., Yapici S. and Arzutug, M. E., Pressure drop and point mass transfer in a rectangular microchannel, *International Communications in Heat and Mass Transfer*, 36, 618 – 623.
- Chen, Y., Zhang, C., Shi, M. and Wu, J., 2009, Three-dimensional numerical simulation of heat and fluid flow in noncircular microchannel heat sinks, *International Communications in Heat and Mass Transfer*, 36, 917 – 920.
- Coetzer, C. B. and Visser, J. A., 2003, Compact modeling of forced flow in longitudinal fin heat sinks with tip bypass, *Journal of Electronic Packaging*, 125, 319 – 324.
- Dogruoz, M. B., Ortega, A. and Westphal, R. V., 2006, A model for flow bypass and tip leakage in pin fin heat sinks, *Journal of Electronic Packaging*, 128, 53 – 60.

- Elshafei E. A. M., 2007, Effect of flow bypass on the performance of a shrouded longitudinal fin array, *Applied Thermal Engineering*, 27, 2233 – 2242.
- Garcia-Hernando, N., Acosta-Iborra, A., Ruiz-Rivas, U. and Izquierdo, M., 2009, Experimental investigation of fluid flow and heat transfer in a single-phase liquid flow micro-heat exchanger, *International Journal of Heat and Mass Transfer*, 52, 5433 – 5446.
- Garimella, S. V. and Singhal V., 2004. Single-phase flow and heat transport and pumping considerations in microchannel heat sinks, *Heat Transfer Engineering*, 25, 1, 15 – 25.
- Harms, T. M., Kazmierzak, M. J. and Gerner, F. M., 1999, Developing convective heat transfer in deep rectangular microchannels, *International Journal of Heat and Fluid Flow*, 20, 149 – 157.
- Holman, J. P., 1992, *Heat Transfer* (Seventh Ed.), McGraw-Hill, Singapore.
- Jeng, T. M. , 2008, A porous model for the square pin-fin heat sink situated in a rectangular channel with laminar side-bypass flow, *International Journal of Heat and Mass Transfer*, 51, 2214 – 2226.
- Jung, Y. M., Seok, P. J. and Sung, J. K., 2004, Effect of tip clearance on the cooling performance of a microchannel heat sink, *International Journal of Heat and Mass Transfer*, 47, 1099 – 1103.
- Kandlikar, S. G., 2006 Single-phase liquid flow in minichannels and microchannels, *Heat Transfer and Fluid Flow in Minichannels and Microchannels*, 87 – 136.
- Khan, W. A. and Yovanovich, M. M., 2007, Effect of bypass on overall performance of pin-fin heat sinks, *J. of Thermophysics and Heat Transfer*, 21, 562 – 567.
- Koo, J. and Kleinstreuer, C., 2004, Viscous dissipation effects in microtubes and microchannels, *International Journal of Heat and Mass Transfer*, 47, 14-16, 3159-3169.
- Lee, P. S., Garimella, S. V. and Liu, D., 2005, Investigation of heat transfer in rectangular microchannels, *International Journal of Heat and Mass Transfer*, 48, 1688 – 1704.
- Li, H. Y., Tsai, G. L., Chiang, M. H. and Lin, J. Y., 2009, Effect of a shield on the hydraulic and thermal performance of a plate-fin heat sink, *Int. Comm. in Heat and Mass Transfer*, 36, 233 – 240.
- Moores, K. A., Kim, J. and Joshi Y. K., 2009, Heat transfer and fluid flow in shrouded pin fin arrays with and without tip clearance, *International Journal of Heat and Mass Transfer*, 52, 5978 – 5989.
- Naphon, P. and Sookkasem, A., 2007 Investigation on heat transfer characteristics of tapered cylinder pin fin heat sinks, *Energy Conversion and Management*, 48, 2671 – 2679.
- Park H. S. and Punch, J., 2008 Friction factor and heat transfer in multiple microchannels with uniform flow distribution, *Int. Journal of Heat and Mass Transfer*, 51, 4535 – 4543.
- Sara, O. N., Barlay Ergu, O., Arzutug, M. E. and Yapici, S., 2009, Experimental study of laminar forced convective mass transfer and pressure drop in microtubes, *Int. Journal of Thermal Sciences*, 1 – 7.
- Sata, Y., Iwasaki, H. and Ishizuka, M., 1997 Development of prediction technique for cooling performance of finned heat sink in uniform flow, *IEEE Transactions On Components, Packaging, And Manufacturing, Part A*, 20, 160 – 166.
- Shokouhmand, H., Ghazvini, M. and Shabaniyan, J., 2008, Analysis of Microchannel Heat Sink Performance Using Nanofluids in Turbulent and Laminar Flow Regimes and Its Simulation Using Artificial Neural Network, *Computer Modeling and Simulation 2008 (UKSIM 2008) Tenth International Conference*, 623 – 628.
- Steinke, M. E. and Kandlikar, S. G., 2006, Single-phase liquid friction factors in microchannels, *International Journal of Thermal Sciences*, 45, 1073 – 1083.
- Tuckerman, D. B. and Pease R. F. W.; 1981, High performance heat sinking for VLSI, *IEEE Electron Device Lett. ELD-2*, 5, 126-129.
- Xie, X. L., Liu, Z. J., He, Y. L. and Tao, W. Q., 2009, Numerical study of laminar heat transfer and pressure drop characteristics in a water – cooled minichannel heat sink, *Applied Thermal Engineering*, 29, 64 – 74.